

A SIMPLIFIED CLOSE RANGE PHOTOGRAMMETRY METHOD FOR SOIL EROSION ASSESSMENT

Sayjro Nouwakpo, Purdue University, W. Lafayette, IN, snouwakp@purdue.edu
Chi-hua Huang, USDA-ARS, W. Lafayette, IN, chi-hua.huang@ars.usda.gov
Jim Frankenberger, USDA-ARS, W. Lafayette, IN, Jim.Frankenberger@ars.usda.gov
James Bethel, Purdue University, W Lafayette, IN, bethel@purdue.edu

Abstract With the increased affordability of consumer grade cameras and the development of powerful image processing software, digital photogrammetry offers a competitive advantage as a tool for soil erosion estimation compared to other technologies. One bottleneck of digital photogrammetry is its dependency on accurately measured control points, which are usually obtained using survey grade equipment such as RTK-GPS. Also, even though many soil erosion studies have used digital photogrammetry for soil erosion assessments; little studies have compared this technology to any other technologies. In this paper, we propose a digital photogrammetry method for control points coordinates acquisition without the need of any survey grade equipment. The method, based on a constrained bundle block adjustment, was successfully tested on a 2m x 2m soil box. We obtained high quality control points with a Length Measurement Error of 1.3×10^{-3} m and mean deviations from the different axes obtained were $S_X = \pm 0.011$ m/m, $S_Y = \pm 0.009$ m/m and $S_Z = \pm 0.002$ m/m. We also present in this paper an extensive comparison between laser scanner technology and digital photogrammetry in producing DEMs and detecting soil surface elevation changes. We found that the agreement between Digital Elevation Models (DEM) from both technologies improved as the soil surface became smoother and the amount of soil loss increased. Our results suggest that digital photogrammetry is suitable for field applications such as gully geometry measurement, erosion measurement on highly eroding areas, stream bank erosion, and gully headcut evolution, etc.

INTRODUCTION

Soil loss after an erosive event is a variable of high interest in soil erosion research. Important soil properties such as erodibility and critical shear stress are derived from soil loss measurements. One widely used technique to quickly assess soil erosion in the field is the erosion pins method (Hudson et al, 1993) in which, pins of known length are driven in the soil before an erosive event. The change in elevation of the exposed part of the pin after the erosive event indicates the amount of erosion that has occurred. The accuracy of this technique is however limited by the low spatial resolution that is in practice attainable (Hudson et al, 1993).

Scientists have applied various technologies to acquire detailed soil elevation data to quantify surface boundary processes, such as erosion. Elliot et al. (1997) used a mechanical relief meter to obtain rill geometry. This technique requires a contact between the measuring device and the soil, which may undergo disturbances as a result. Non-contact soil surface elevation measurement technologies, such as laser scanning and stereo-photogrammetry, are preferred. While laser technology is the most accurate, stereo-photogrammetry has the advantage of having a lower initial cost, due to advances in digital imaging technology.

Stereo-photogrammetry has long been used to assess land degradation (e.g., Warner and Reutebuch, 1999), measure soil erosion (e.g., Pyle et al, 1997; Rieke-zapp and Nearing, 2005; Abd Elbasit et al., 2009) or estimate soil roughness (e.g., Merel and Farres, 1998). One of the main advantages of stereo-photogrammetry is that it has been simplified over the years with the development of good quality consumer grade digital cameras and powerful image processing and camera calibration algorithms.

While the steps involved in the image processing and camera calibration have been simplified considerably, this technology still relies on the acquisition of accurately measured control points. Various procedures have been proposed to alleviate the workflow required by the field survey steps. Warner and Reutebuch (1999) proposed a dual camera system with a fixed base which allows performing the photogrammetric measurements in a relative coordinate without the need of measured control points. Rieke-zapp et al. (2009) mapped rock outcrops in the field using only a laser ruler as survey equipment. Their method uses an arbitrary coordinate system and known distances from the scene to determine the camera positions and derive a Digital Elevation Model (DEM).

The objectives of this paper are to: (1) present a single camera stereo-photogrammetric approach for soil surface measurements that can be easily deployed without the need of additional survey equipments while preserving the absolute horizontal and vertical orientation of the scene; and (2) assess the accuracy and the sensitivity of stereo-photogrammetry in detecting changes in soil surface elevation by comparing DEMs with those obtained from a laser scanner technology.

MATERIALS AND METHODS

A Photogrammetric Approach For Control Point Measurement In this section, we propose a procedure to accurately obtain the coordinates, or XYZ positions, of signalized control points without the need of any survey equipment. We achieved this, by developing an independent photogrammetric approach that uses known information about the object space to compute the relative position of the signalized control points. Object space information used in this procedure includes parallelism between lines, known distances and elevation difference between points. This information is incorporated in a bundle block adjustment as a set of constraint equations to determine the XYZ positions of the signalized control points. A bundle block adjustment or block triangulation is the most economical photogrammetric approach for yielding accurate and consistent mapping (Mikhail et al., 2001).

A typical workflow in a photogrammetric bundle block adjustment requires initial approximation for the exterior orientation parameters (Linder, 2009). On one hand, while it is relatively easy to assume reasonable initial values for exterior orientation parameters of nadir looking images, it is more challenging to obtain decent initial approximations for arbitrarily oriented images. On the other hand, arbitrarily oriented pictures are easier to obtain than vertical images.

Our goal was to develop a technique that is practical to use; therefore, we developed an algorithm that made it possible to take arbitrarily oriented images and still find reasonable approximations of their exterior orientations. The algorithm was based on the work of Heuvel (1997) that uses parallel lines in the scene to retrieve the exterior orientation of the camera. The

advantage of this algorithm is that it allows a direct determination of the exterior orientation parameters. These exterior orientation values can be refined in a subsequent bundle block adjustment.

In order to obtain the XYZ positions of the control points at a high degree of accuracy, we wrote a bundle block adjustment program that requires a set of constraints. We provided measured distances in the scene as well as known elevation differences between points. The constraints were introduced in the bundle block system using Helmert's method (Mikhail et al., 2001) in which the constraint equations border the reduced normal equations.

Test Procedure We conducted the testing on a 2m x 2m soil box. The camera used was a Single Lens Reflex (SLR) Canon EOS Digital Rebel XT with an 8 megapixel sensor and a 20mm lens mounted on it. To obtain a uniform DEM resolution, we used nadir looking images for the DEM extraction process. These vertical pictures were taken by mounting the camera on a transverse aluminum beam. The beam was located approximately at 1.5m above the soil box and was supported by two ladders at each end of the soil box.

We custom made signalized target points from cylindrical aluminum bars cut in small pieces. To make the image points collection as precise as possible, a crosshair sign was glued at the top of each target point. The image coordinate of the target was collected by pointing the cursor on the crosshair sign. The targets were identified by numbers visible on every image. To assure that the targets will not be moved or disturbed by the eroding soil, each target was anchored in the soil by a 5×10^{-2} m nail glued at its bottom.

In order to directly determine the exterior orientation parameters using the parallel lines approach, we built a 0.5 m by 0.5 m rectangular frame. The rectangular frame was used because it not only provided the parallel lines needed but also the 90 degree angles which were convenient in defining a Cartesian datum. To further constrain the bundle block adjustment, we used 2 rigid aluminum bars with markers of known distances on each bar.

To assess the accuracy and the sensitivity of the photogrammetry technique, we compared a DEM obtained from the photogrammetry approach to a DEM obtained from a laser scanner. The laser scanner that we used was developed by Darboux and Huang (2003). It is a triangulation based laser scanner that converts the relief displacement observed on a laser line into point elevation. It can scan a surface at a spatial resolution of 0.75×10^{-3} m by 2.75×10^{-3} m with an elevational accuracy of 0.5×10^{-3} m.

Workflow and Software We calibrated the camera using the Matlab Calibration Toolbox by Jean-Yves Bouquet. The internal camera parameters were computed based on the work of Heikkilä and Silvén (1997). The camera was set on manual mode before calibration and the distance setting kept unchanged during all experiments.

To implement the proposed photogrammetric approach, we start by arranging the control point uniformly across the soil box. The nails at the bottom of the control points were driven deep into the soil to assure that the control points were stable and could be used for successive erosive events.

The rectangular frame was placed in the middle of the soil box to assure uniform error propagation. The frame was leveled using a digital level so that the Z coordinate of all the four points of the rectangle can be set to zero. The rigid bars were also leveled across the soil box to provide constraint equation on both distance and elevation between the 2 marked points on each bar. Figure 1 shows the entire setup ready to be photographed.



Figure 1 Soil box setup with rectangular frame and aluminum bars.

Once the control points, rectangular frame and bars were setup, a series of four or more pictures of the scene were taken with a full overlap of the soil box. The pictures were taken with the camera handheld from each corner of the soil box. The optical axis was at approximately 45° from the vertical axis. The image converging configuration increased the geometric stability of the bundle block adjustment.

After the series of pictures were taken, we removed the rectangular frame as well as the rigid bars from the scene. Removing the frame and the level bars minimized artificially induced objects on the soil surface. The camera was then mounted on the transverse beam and a strip of 7 pictures was taken with a 65% forward overlap. Three strips covered the entire soil box with approximately 53% side overlap.

After all the pictures were taken, they are split into 2 groups and processed differently. The first set of images, called survey images, contained all the oblique images that were intended to retrieve the XYZ location of the control points. All survey images had the rectangular frame in the middle of the scene. The second set of images that we called the DEM images were the nadir looking images.

The image coordinates of all the interest points in the survey images were collected using ImageJ, a Java based image processing and analysis software. Once collected, the image coordinates were input into a program that we wrote in Matlab. The program included a subroutine for the direct determination of the exterior parameters and a bundle block adjustment script. The bundle block adjustment iterates until the different rays that determine a point

converging to a stable position (Fig 2). The outputs of the program include the XYZ coordinates of the control points, the exterior orientation parameters and the residuals of the bundle block adjustment.

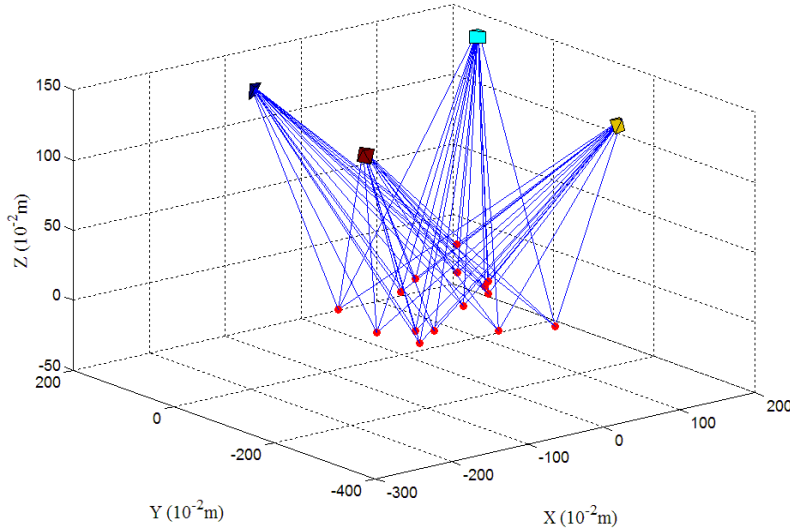


Figure 2 Ray intersections using the constrained bundle block adjustment.

Once the XYZ coordinates of all the control points of the scene were determined, they were imported into the image processing software Leica Photogrammetry Suite (LPS) along with the DEM images. The DEM was then created according to the LPS DEM extraction procedure. Figure 3 shows a DEM of the soil box produced with LPS.

Measurement Accuracy We measured the accuracy of the XYZ coordinates of the control points obtained from the survey images by including check points in the bundle block adjustment. The check points were arranged by pairs on plumb lines across the soil box. A pair of points was located on an independently leveled bar. The distance between the points forming each pair was carefully measured with a ruler and compared with the length obtained from the XYZ output of the bundle block adjustment. Arranging the points on plumb lines and on level bars allowed assessing not only the length accuracy of the photogrammetry technique but it also provided a mean to verify that the computed coordinates are properly oriented. We estimated the length accuracy by calculating the mean Length Measurement Error (LME) using the following formula:

$$LME = \sqrt{\frac{\sum_{i=1}^n (L_i - L_{m_i})^2}{n}} = \sqrt{\frac{\sum_{i=1}^n (\sqrt{\Delta X_i^2 + \Delta Y_i^2 + \Delta Z_i^2} - L_{m_i})^2}{n}} \quad (1)$$

where ΔX , ΔY , and ΔZ are the differences between the coordinates of each pair of points involved in the length measurement, L_m is the measured length, L is the slope length obtained from the output coordinates, n is the number of pairs of points available.

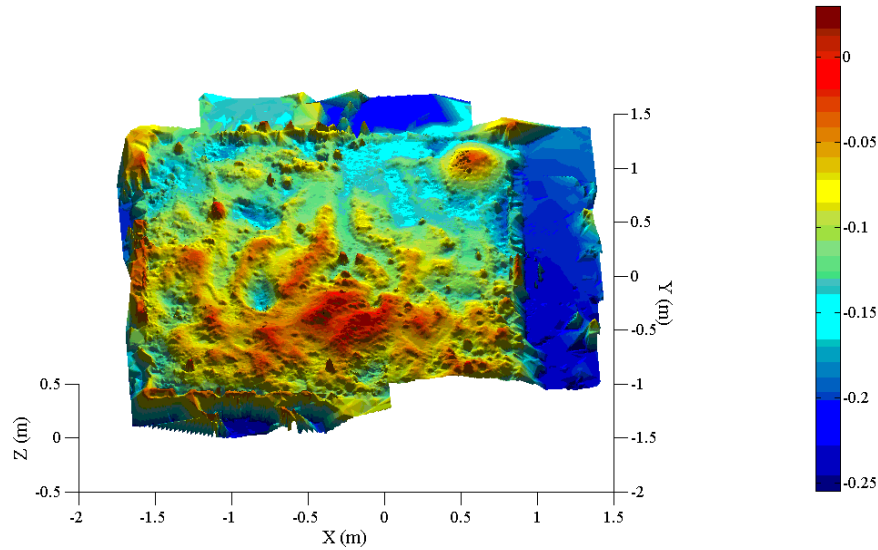


Figure 3 DEM of the soil box obtained using LPS (6×10^{-3} m grid spacing).

To verify that the computed coordinates are properly oriented, we calculate the deviation from the different axes in terms of a slope. A pair of points located on the same plumb line should have the same X and the same Y . Likewise, a pair of points on a leveled bar should have the same elevation Z . We express the accuracy of the orientation in terms of the slope of the deviation from each respective axis. From the plumb lines, we can obtain the deviation from the X and Y axes.

$$S_X = \sqrt{\frac{1}{n_1} \sum_{i=1}^{n_1} \left(\frac{\Delta X_i}{L_i} \right)^2}, S_Y = \sqrt{\frac{1}{n_1} \sum_{i=1}^{n_1} \left(\frac{\Delta Y_i}{L_i} \right)^2} \quad (2)$$

where n_1 is the number of plumb lines available.

From the leveled bars, we can obtain the deviation from the Z axis by

$$S_Z = \sqrt{\frac{1}{n_2} \sum_{i=1}^{n_2} \left(\frac{\Delta Z_i}{L_i} \right)^2} \quad (3)$$

where n_2 is the number of leveled bars available.

To assess the accuracy of the digital photogrammetry technology in measuring soil surface elevation, we compared the DEM obtained from the digital photogrammetry technique to the DEM obtained from a laser scanner. The sensitivity of digital photogrammetry in measuring soil erosion was assessed by subjecting the soil box to 2 successive rainfall events. Both rainfalls were 1hr long but the first rainfall had an intensity of 25mm/h while the second rainfall had an intensity of 50mm/hr.

The microtopography of the soil box was measured after each rainfall event using the laser scanner and digital photogrammetry. The elevation change was calculated by subtracting the DEM before the erosive event from the DEM after the erosive event. The resulting spatial elevation changes obtained from laser scanner and digital photogrammetry were then compared.

To compare the laser scanner to the digital photogrammetry, all the DEMs had to be registered to the same coordinate system. To do so, we extracted a point cloud making up 3 non collinear target points and ran a rigid point cloud registration. For the registration, we used a Coherent Point Drift algorithm (Myronenko and Song, 2009) which considers the alignment of two point sets as a probability density estimation problem.

The DEM comparison was made at a 6.0×10^{-3} m grid spacing, which was the minimum resolution attainable by the photogrammetric configuration. The Laser scanner DEMs had to be re-sampled from a 2.75×10^{-3} m grid to 6.0×10^{-3} m grid. At this spatial resolution, the DEM provided 38465 comparison points. To the best of our knowledge, this was the first time that such an extensive comparison of the laser scanner and digital photogrammetry was performed. An earlier study by Rieke-Zapp et al. (2001) compared relative accuracies of both technologies, but they did not make a point-to-point DEM comparison. Recently, Aguilar et al. (2009) compared elevation values obtained from both technologies but their study area was 20 times smaller than the one we are testing in this paper (0.2 m^2 vs. 4 m^2).

RESULTS AND DISCUSSIONS

Determination the XYZ Coordinates of Control Points We successfully determined the XYZ location of the control points using the constrained bundle block adjustment. The Root Mean Square Error (RMSE) of the image coordinate residuals was 0.91 pixel. With an average scale of 144.8, we estimated the ground coordinate precision to be 0.83×10^{-3} m. Table 1 summarizes the accuracy test performed on the check points. The LME obtained from the check points was 1.3×10^{-3} m. The mean deviations from the different axes obtained were $S_X = \pm 0.011 \text{ m/m}$, $S_Y = \pm 0.009 \text{ m/m}$ and $S_Z = \pm 0.002 \text{ m/m}$.

Most survey grade RTK GPS receivers have horizontal and vertical accuracies to the order of 10^{-2} m and 2×10^{-2} m respectively (Trimble Navigation, Ltd., 2002). In our photogrammetric approach, we were able to determine XYZ location for control points at the same level of accuracy as RTK GPS systems. It is also important to note that because we used convergent images for the bundle block adjustment, our local accuracy in the vertical direction was approximately 10 times better than that obtained from RTK GPS.

For small scale project such as laboratory conditions where GPS signal might be weakened or small field plots ($\sim 3\text{m} \times 3\text{m}$), the photogrammetric approach that we propose presents the advantage to be highly accurate and easy to deploy. It is possible to use this approach on an area larger than the one tested in this paper. Doing so would however require a segmentation of the entire area in smaller sub-areas which can be tied together through common border points. The main danger of such setup is that it can lead to a deformed model.

Table1 Accuracy of the photogrammetric approach in determining XYZ of check points.

	X (10 ⁻² m)	Y (10 ⁻² m)	Z (10 ⁻² m)	L (10 ⁻² m)	L _m (10 ⁻² m)
Plumb line1	53.444	-29.314	5.842	19.921	19.792
	53.510	-28.990	25.760		
Plumb line2	45.732	-102.936	1.075	9.035	9.000
	45.872	-102.942	10.109		
Plumb line3	-74.084	-139.624	-6.112	37.504	37.503
	-74.449	-139.632	31.390		
Leveled bar	-111.890	-41.520	-7.161	179.574	179.800
	-14.779	-192.570	-7.588		

Digital Photogrammetry Versus Laser Scanner Figure 4 show plots of elevations (Z values) of the photogrammetry DEM against those obtain from laser scanning. The comparisons were made before any erosive event (Fig 4-a), after a 25 mm/hr rainfall (Fig 4-b) and after 50 mm/hr rainfall (Fig 4-c).

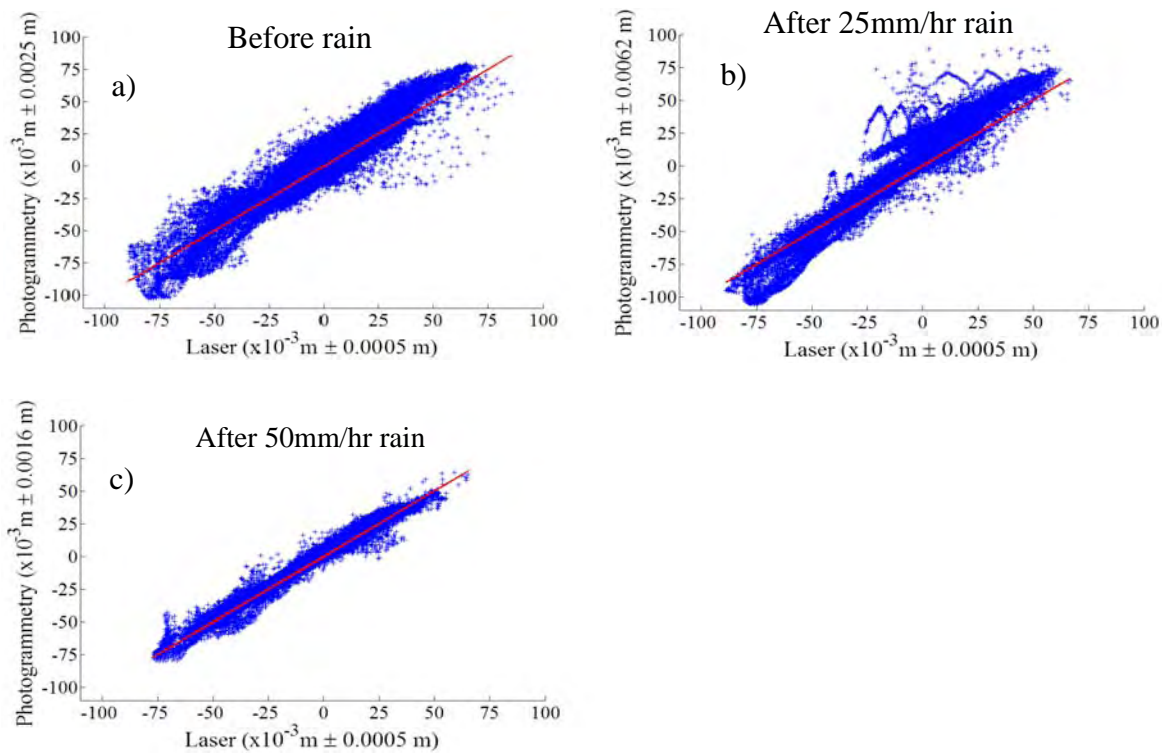


Figure 4 Photogrammetry vs. laser scanner DEM comparison.

In the ideal case, the Z values of both technologies should follow closely the 1-1 line. From the plot, it appears that the width of the error band around the 1-1 line reduces after successive

erosion of the soil. On Fig 4b, we can observe a systematic deviation from the 1-1 line and the presence of a repetitive sinusoidal error pattern.

Several sources of errors explain the deviation from the 1-1 line. Errors in the photogrammetric DEM are mainly due to image point matching errors. In the laser scanner Dem, the main source of error is due to missing data because of hidden point from the laser scanner camera view. These missing points were linearly interpolated; creating the sinusoidal pattern observed in Fig 4-b.

The width of the error band was larger on the rough surface because both technologies are affected by surface roughness. Rough surfaces present more localized relief displacement, which in turn tend to reduce the performance of the photogrammetry image matching algorithm. The laser scanner technology is also affected by surface roughness because more laser points are shaded by large soil clods. As the soil erodes after successive rainfalls, its surface becomes smoother, reducing DEM errors. Aguilar et al. (2009) also found similar results when comparing DEMs from laser scanner and photogrammetry.

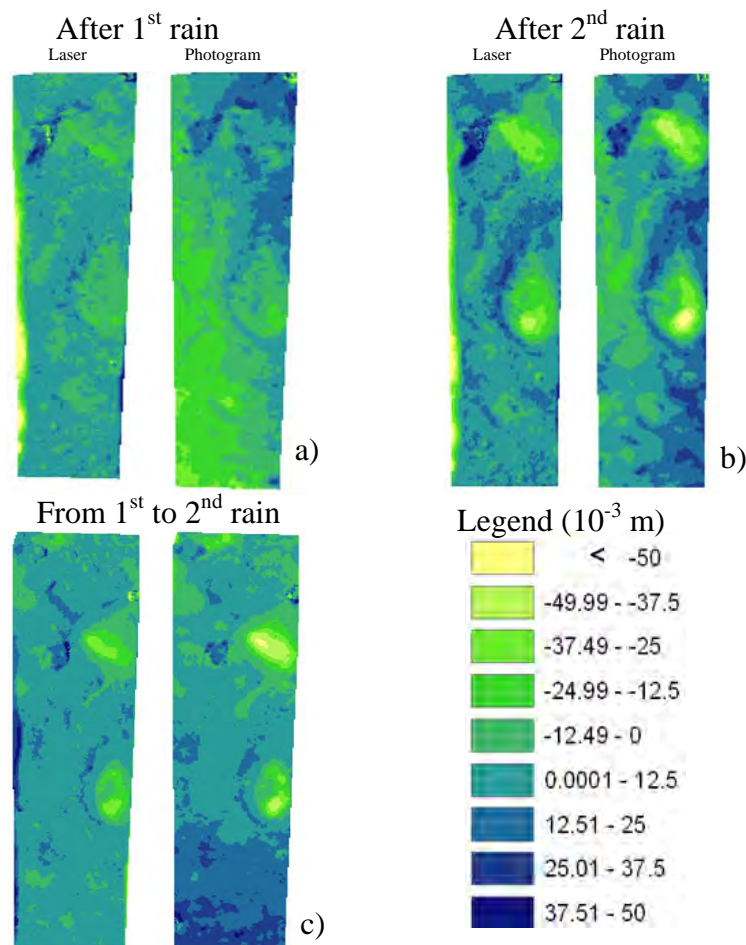


Figure 5 Elevation change map (6×10^{-3} m grid spacing).

Figure 5 shows the spatial distribution of elevation changes predicted by laser scanner and digital photogrammetry approaches. The elevation change after the first rain (25mm/hr), and the second rain (50mm/hr) were mapped on Fig 5-a and Fig 5-b respectively. Fig 5-c mapped the elevation change that occurred from the first rain to the second rain. The negative values in the legend represent deposition areas and the positive values represent erosion areas. Despite its inherent errors, the photogrammetry DEM was able to detect surface elevation changes. The agreement between laser scanner and photogrammetry is improved with successive rainfalls.

Results from comparing elevation change confirmed the earlier findings in comparing DEMs. Estimated elevation changes agreed better after the more intense 50 mm/h storm than after the initial 25mm/hr rainfall between the 2 technologies. Both techniques seem to work better on smooth surfaces than on irregular surfaces. Applications suitable for the photogrammetric technology include ephemeral gully geometry measurement, erosion measurement on highly eroding areas such as stream bank erosion, and gully headcut evolution, etc.

CONCLUSION

Using the proposed photogrammetric approach, we successfully obtained accurate XYZ positions of control points without needing any survey grade equipment. On a 2m by 2m plot, the accuracy of the control points was similar to that of a survey grade GPS unit. Our work suggests that using a photogrammetric approach to acquire coordinates of control points is convenient for small scale projects (~3m x 3m). Even though it is possible to apply this method to a larger area, care has to be taken to not deform the geometric model. We have successfully tested our approach both in laboratory and in the field.

In this paper, we had the opportunity to compare DEMs acquired from the photogrammetry technology to those obtained from detailed laser scanning. This was the first time that such an intensive comparison of both technologies was done. We found that image point matching errors in the photogrammetry technology and missing point in the laser scanner data were the main sources of deviations. We also found that the agreement between the 2 technologies improved as the soil surface became smooth after successive rainfall events.

REFERENCES

- Abd Elbasit M. A., Anyoji H., Yasuda H., Yamamoto S. (2009). "Potential of low cost close-range photogrammetry system in soil microtopography quantification," *Hydrological Processes*, 23(10), pp 1408–1417.
- Aguilar M. A., Aguilar M. J., Negreiros J. (2009). "Off-the-shelf laser scanning and close-range digital photogrammetry for measuring agricultural soils microrelief," *Biosystems Engineering*, 103(4), pp 504–517
- Darbox F., Huang C. (2003). "An instantaneous-profile laser scanner to measure soil surface microtopography," *Soil Science Society of America Journal*, 67, pp 92–99.
- Elliot W. J., Laflen J. M., Thomas A. W., Kohl K. D. (1997). "Photogrammetric and rillmeter techniques for hydraulic measurement in soil erosion studies," *Transactions of the ASAE*, 40(1), pp 157–165.

- Heikkilä J., Silvén O. (1997). "A four-step camera calibration procedure with implicit image correction," IEEE Computer Society Conference on Computer Vision and Pattern Recognition, San Juan, Puerto Rico, pp 1106–1112
- Hudson N. W. (1993). *Field Measurement of Soil Erosion and Runoff*. Silsoe Associates Ampthill, Bedford United Kingdom.
- Linder W. (2009). *Digital Photogrammetry A Practical Course*. Springer Berlin, Heidelberg.
- Merel A. P., Farres P. J. (1998). "The monitoring of soil surface development using analytical photogrammetry," *Photogrammetric Record*, 16(92), pp 331–345.
- Mikhail E. M., Bethel J. S., McGlone J. C. (2001). *Introduction To Modern Photogrammetry*. John Willey and Sons, Inc., New York.
- Myronenko A., Song X. (2009). "Point set registration: coherent point drift," Technical Report arXiv:0905.2635v1.
- Pyle C. J., Richards K. S., Chandler J. H. (1997). "Digital photogrammetric monitoring of river bank erosion," *Photogrammetric Record*, 15(89), pp 753–764.
- Rieke-Zapp D. H., Nearing M. A. (2005). "Digital close range photogrammetry for measurement of soil erosion," *Photogrammetric Record*, 20(109), pp 69–87.
- Rieke-Zapp D. H., Rosenbauer R., Schlunegger F. (2009). "A photogrammetric surveying method for field applications," *The photogrammetric Record*, 24(125), pp 5–22.
- Rieke-Zapp D. H., Wegmann H., Santel F., Nearing M. A. (2001). "Digital photogrammetry for measuring soil surface roughness," *Proceedings of the American Society of Photogrammetry and Remote Sensing 2001 Conference: Gateway to the New Millenium*, St Louis, Missouri, pp 1–8
- Trimble Navigation, Ltd. (2002) *Mapping Systems General Reference*. Trimble Navigation, Ltd. Sunnyvale, California.
- Van den Heuvel F. A. (1997). "Exterior orientation using coplanar parallel lines," *Proceedings of the 10th Scandinavian Conference on Image Analysis*, Lappeenranta, pp 71–78.
- Warner W. S., Reutebuch S. E. (1999). "Application and accuracy of two fixed base camera systems," *Photogrammetric Record*, 16(93), pp 423–432.